

AC-coupled GaAs microstrip detectors with a new type of integrated bias resistors

R. Irsigler¹, R. Geppert, R. Göppert, M. Hornung, J. Ludwig,
M. Rogalla, K. Runge, Th. Schmid, A. Söldner-Rembold,
M. Weibel, C. Weber

*Albert-Ludwigs-Universität Freiburg, Fakultät für Physik,
D-79104 Freiburg, Germany*

Full size single-sided GaAs microstrip detectors with integrated coupling capacitors and bias resistors have been fabricated on 3" substrate wafers. PECVD deposited SiO₂ and SiO₂/Si₃N₄ layers were used to provide coupling capacitances of 32.5 pF/cm and 61.6 pF/cm, respectively. The resistors are made of sputtered CERMET using simple lift off technique. The sheet resistivity of 78 kΩ/sq. and the thermal coefficient of resistance of less than 4×10⁻³/°C satisfy the demands of small area biasing resistors, working on a wide temperature range.

1 Introduction

Several aspects on the design of a semiconductor microstrip detectors has to be taken into account in order to get a good signal to noise ratio. First of all, the strip capacitance (the sum of the interstrip capacitances between neighbouring strips and the body capacitance of the strip) should be low because it determines the noise level of the readout electronics [1]. For short shaping times, there is almost no additional contribution due to the shot noise of the detector. This is still the case for the higher leakage currents of GaAs detectors (~ 20 nA/mm²) [2] compared to standard Si detectors (~ 0.5 nA/mm²) [3]. Short shaping times have to be used because of the very high luminosity (10^{34} cm⁻²s⁻¹) and high bunch crossing rate (40 MHz) at future high energy physics experiments like LHC [4].

¹ Corresponding author, Tel.: +49 761 203 5911, fax: +49 761 203 5931, e-mail: irsigler@ruhpb.physik.uni-freiburg.de

Secondly, the interstrip capacitance has to be large compared to the body (backplane) capacitance of the strip to avoid signal losses to ground.

Thirdly, the coupling capacitance has to be magnitudes higher compared to the strip capacitance in order to avoid a signal spreading to neighbouring strips [5].

Biasing resistors are necessary to drain out the leakage current of the detector. In conjunction with the strip capacitors, they act as a low pass filters. Values in the range of $M\Omega$ are needed to avoid signal losses to ground.

In addition strip resistance has to be minimized to reduce dispersion of the signal pulse during penetration at the transmission line of the strip [6].

Due to limited space resources, it is not possible to integrate coupling capacitors and bias resistors on VLSI-amplifier chips. Hence external capacitor and resistor chips have to be used, or they have to be integrated onto the detector. On integrated detectors, a reduced number of interconnections have to be made which improves yield and reliability. On the other hand additional processing steps raise cost and complexity of detector fabrication.

Simplification of processing steps is an essential task in detector design. One of the major advantages of GaAs detectors is the fact that simple Schottky contacts can be used instead of diffused or implanted pn-contacts in silicon technology. No intermediate p-stops are needed to compensate accumulated surface charge between n-strips. Although GaAs substrate wafers are more expensive than Si wafers, a reduced number of masks and processing steps makes GaAs microstrip detectors competitive to standard Si-detectors.

The design, fabrication and electrical performance of integrated GaAs-microstrip detectors are described in the following sections.

2 Wafer design

The wafer design contains several detectors and test structures. In accordance to the SCT96 layout specification of the ATLAS detector at LHC [7], a keystone detector was designed which covers the main part of the wafer. The 6 cm long detector with 256 strips has a tilt angle of 3° and a varying pitch from $80\ \mu\text{m}$ at the top to $68\ \mu\text{m}$ at the bottom of the strips. The gap between the strips is constantly $25\ \mu\text{m}$. At the bottom, each strip is connectet via a biasing resistor to the common bias bar.

In addition, four detectors with a reduced lenght of 1.5 cm, $50\ \mu\text{m}$ pitch and 256 strips were placed on the wafer design. Two of them are detectors with

a variable width of the strips (40/30/25/20 μm) which are grouped in 64 strips each. All detectors are AC-coupled. The detectors are surrounded with some test structures to measure the performance of the biasing resistors and coupling capacitances.

The mask set consists of six layers. The first one defines the strips, guard ring, bond pads and biasing line of the detector. The second mask opens the contact windows for the bond pads and the resistors in the dielectric layer. The third mask is used for the CERMET resistors. The resistor lines lay on top of the dielectric and are connected to the strips and the common biasing line via etched holes. The serpentine design was selected because of a better utilisation of the area. The fourth mask defines the top strip metallization for the capacitors and provides vias over the guard ring to the bond pads at the first level metallization. Mask five and six define the backside metallization of the wafer and opens contact holes in the backside passivation.

Fig.1 shows the integrated CERMET resistors at the end of a 50 μm pitch microstrip detector. The strips are surrounded by a guard ring.

3 Device fabrication

All detectors have been designed and fabricated in our laboratory at the Materials Research Center in Freiburg. Detectors and test structures of various geometries were processed on 3 in. semi insulating GaAs from Freiberger Compound Materials. Before deposition of the contacts, wafers were cleaned in acetone and iso-propanol with a subsequent etch in HCl/H₂O and NH₄OH/H₂O₂/H₂O. Either Ti/Pt/Au/Ni (10/20/80/5 nm) or Ti/Ti-W/Al/Ti-W (10/10/100/5 nm) layers were used as first level metallization. Depending on the barrier layer, the Schottky contacts are stable up to process temperatures between 400 °C and 500 °C. RBS measurements have shown that the sputtered Ti-W barrier layer exhibits a better performance with respect to the temperature stability of the Schottky contact. In either case thermal budget is a critical point during detector fabrication. The strip resistance was in the range between 150 Ω/cm and 200 Ω/cm for 30 μm wide Strips.

Single layers of SiO₂ or double layers of SiO₂/Si₃N₄ were deposited at 300°C in a PECVD process. Afterwards contact holes were etched into the dielectric layers to provide interconnections to the resistors and the second level metallization (see Fig. 2). The etch mask was also used for a Ni/Au/Ni (10/90/10 nm) plug fill of the contact holes. In the next step, CERMET was sputtered onto the wafer to define the resistors after the lift off process. Then, the second level metallization was deposited using either evaporated Ni/Au (10/100 nm) layers or sputtered Al (120 nm) to provide the coupling capacitors.

Next, the front side was covered with photoresist to protect the surface and the originally 625 μm thick wafers were lapped and polished down in a CMP process to a residual thickness of 200 μm . The backside of the wafers were O-implanted at an energy of 130 keV with a dose of $1 \times 10^{13} \text{ cm}^{-2}$. The resulting damage induced isolation layer improves the breakdown behavior at full depletion [8]. Afterwards, the backside was patterned photolithographically in a double sided mask aligner to define the backside contact under the strips. Sputtered Ti-W/Al (10/120 nm) was used as metallization. Finally a layer of PECVD SiO_2 was deposited and etched to protect the backside from scratches during handling and mounting of the detectors.

4 Interstrip capacitance

Variation of the interstrip capacitance with the gap was measured at the variable width detector. As expected, the interstrip capacitance is a decreasing function with the separation of the strips. As shown in Fig.3, the interstrip capacitance to the first neighbour strip varies between 1.15 pF/cm at 10 μm separation down to 0.67 pF/cm for a gap of 30 μm . The interstrip capacitance to the second neighbour strip is about 60 % of this. Hence a total strip capacitance in the range between 2.5 pF/cm and 4.5 pF/cm could be expected for the considered detector geometries. Demanding a ten times higher coupling capacitance, the coupling capacitance should be in the range between 150 pF and 270 pF for 6 cm long strips.

5 Coupling capacitors

Because of the poor electric properties of native GaAs oxides (As_2O_3 , Ga_2O_3), foreign dielectric materials have to be used in GaAs device processing. Materials available for dielectric layers in microelectronics are usually SiO_2 , Si_3N_4 , Al_2O_3 , Ta_2O_5 and Polyimide [9]. All of those materials are showing some strengths and weaknesses.

Depending on the deposition technique and conditions the dielectric constant is between 4 and 5 for SiO_2 and between 6 and 9 for Si_3N_4 . Usually they are deposited in a PECVD process at relatively low temperatures (300 $^\circ\text{C}$). Both layers are easily wet etchable in buffered HF to open contact windows. A combination of both layers are often preferred because of the lower breakdown voltage due to pinholes formation in SiO_2 and the high intrinsic stress of Si_3N_4 when single layers are used [10].

Polyimide can be easily spun onto surfaces like a photoresist but require high

curing temperatures ($> 400\text{ }^\circ\text{C}$) to achieve best dielectric properties. Dielectric constant is in the range between 3 and 4. Film thickness is hard to control and patterning has to be done using dry etching in an oxygen plasma [9].

Al_2O_3 and Ta_2O_5 have high dielectric constants of 9.5 and more than 20, respectively. Sputtering methods can be used for deposition but surface damage and variation of film thickness can be significant[11].

Within this work, the materials of choice were single layers of SiO_2 (300 nm) and double layers of $\text{SiO}_2/\text{Si}_3\text{N}_4$ (100 nm/200 nm) deposited in a PECVD process. Some results are presented in the following section.

5.1 Measurements

All measurements have been performed on wafer at a probe station using a HP 4284 A LCR-meter in parallel mode. Fixed frequency measurements were done at 10 kHz with a oscillating level of 200 mV and a DC-bias voltage of 2 V in accordance to the expected voltage drop at the biasing resistors.

A comparison between the different dielectric layers is shown in Fig. 4 for a detector with variable strip length and in Fig. 5 for a detector with variable strip width. The calculated dielectric constants for SiO_2 and $\text{SiO}_2/\text{Si}_3\text{N}_4$ are 4.0 and 7.3, respectively. For a strip width of 35 μm , the measured coupling capacitances were 23.0 ± 0.2 pF/cm and 42.0 ± 0.5 pF/cm, respectively. The full size keystone detector with 80 μm pitch, constant gap of 20 μm , constant length of 6 cm and varying width from top to bottom of the strip had a coupling capacitance of 200 pF for SiO_2 and 370 pF for $\text{SiO}_2/\text{Si}_3\text{N}_4$.

As plotted in Fig. 6, the coupling capacitance is frequency independent over a wide range. At frequencies above 100 kHz a significant decrease is observed for the full size keystone detector. This is due to the fact, that the coupling capacitors have to be treated as a distributed transmission line of finite resistors and capacitors[6]. At high frequencies, the effective length of the capacitor is reduced, resulting in a lower capacitance. This is especially the case when implanted strips in Si-detectors have a high resistivity and were not covered with a metallization layer [1]. For the GaAs detector of shorter lengths and smaller resistances, this effect is negligible.

6 Biasing resistors

Using lift-off technique, film thickness is normally restricted to less than 200 nm. In width, the resistor area is restricted by the pitch of the strips. The

length should be as small as possible because it acts as a dead part of the detector. On the other hand, structures become more sensitive to varying deposition conditions if the dimensions are too small. A suitable compromise is a resistor area in the range of $50 \mu\text{m} \times 250 \mu\text{m}$. Hence the sheet resistivity of the resistor material must be in the range of 50 - 100 k Ω /sq. to achieve resistor values in the M Ω range.

Microstrip detectors in the ATLAS-experiment at LHC has to operate at a temperature of -10 °C for a period of at least 10 years. Therefore it is recommended that the resistor material has a low temperature coefficient..

The requirements of a high sheet resistance, long term stability and weak temperature dependence limits the suitable alternatives for resistor materials. Different approaches have been evaluated to integrate biasing structures on microstrip detectors so far. This includes passive components like polysilicon resistors [12] as well as active devices like punch-through biasing [13] and FOXFET structures[14].

Polysilicon has to be deposited at rather high temperatures in a LPCVD process and local implantation steps with post annealing at high temperature has to be applied to get a good ohmic junction at the metal strip/polysilicon interface [15]. Moreover, if pure Al is used as strip metallization, spiking problems could degrade reliability of the resistors.

Punch-through biasing needs no extra processing steps but suffers from a leakage current dependent dynamic resistance which causes considerable base line differences between channels.

On the FOXFET-structure, a gate electrode covering the punch-through gap controls the dynamic resistance. Unfortunately no integration of FOXFET-structures on GaAs detectors is possible because of the well known pinning of the Fermi level to the middle of the band gap at the dielectric/GaAs interface [16]

This work is focussed on a new type of biasing resistors for microstrip detectors which will be discussed in the following section.

6.1 *Integrated CERMET-resistors*

Thin film resistors made of CERMET have been widely used in microelectronic industry for a long time [17] - [21]. CERMET (CERAmic/METal) is a mixture of an insulator (SiO) and a metal (Cr or Au). In this two phase material current transport is interpreted in terms of electron tunneling between metal islands in the insulator matrix [22]. Simultaneously evaporation [23] or sputtering [24]

can be used for deposition.

It was found, that the electrical properties are very sensitive to the CERMET composition and the deposition conditions (substrate temperature, sputtering power, post annealing)[24,21]. Reducing the Cr content in the sputtering target from 50 % to 10 % by volume results in a drastic increase in sheet resistance from $10^3 \Omega/\text{sq.}$ to $10^{13} \Omega/\text{sq.}$. Hence a wide range of resistor values can be obtained by choosing appropriate target composition.

6.2 Measurement

A target composition of 55 Vol. % SiO / 45 Vol. % Cr was chosen in order to reach the mentioned demands on the sheet resistivity. Rf-magnetron sputtering in DC mode have been performed in a sputtering system from von Ardenne (LA250).

Fig. 7 shows the I-V characteristics of the integrated CERMET biasing resistors for two different sputtering powers. In order to achieve a comparable resistor thickness, the sputtering time has to be increased from 100 seconds at 200 Watt to 250 seconds at 100 Watt because of lower deposition rates at reduced power. Adhesion of the CERMET film was found to be excellent in any case. The final thicknesses were measured with a stylus profiler (Tencor P10) giving values of $133 \mu\text{m}$ and $121 \mu\text{m}$ for 200 W and 100 W, respectively. From the slope of the I-V curve, the resistance was calculated to be $4.85 \text{ M}\Omega$ at 200 W and $2.47 \text{ M}\Omega$ at 100 W sputtering power.

Some test vehicles were used to measure the resistance as a function of resistor length. The width of the resistor line was $10 \mu\text{m}$. The corresponding resistivity was calculated to be $0.95 \Omega\text{cm}$ and $3.14 \Omega\text{cm}$ for 100 W and 200 W sputtering power, respectively. This corresponds to a sheet resistance of $78.4 \text{ k}\Omega/\text{sq.}$ and $236 \text{ k}\Omega/\text{sq.}$, respectively.

In steps of 5 K, I-V curves as a function of temperature between $-40 \text{ }^\circ\text{C}$ and $+60 \text{ }^\circ\text{C}$ were measured in a temperature controlled chamber. The temperature behavior is described by the thermal coefficient of resistance (TCR), which is defined as:

$$\alpha = \frac{\Delta R}{R * \Delta T}$$

The TCR α can be calculated from the relative change of resistance $\Delta R/R$ due to a temperature change ΔT . A comparison of the TCR between the

integrated CERMET resistors and an external resistor chip¹ is shown in Fig.8. External R-chips are frequently used, if no biasing resistors are integrated on the detector. In both cases the TCR is negative and smoothly increasing with temperature. For the CERMET resistors a value of $-4 \times 10^{-3}/^{\circ}\text{C}$ at -10°C reaching $-2.5 \times 10^{-3}/^{\circ}\text{C}$ at room temperature was calculated. Those TCR values are even lower than the corresponding values for the external resistors and show the good performance of the CERMET.

Deposition Parameters and resulting resistor values are summarized in Table 1.

6.2.1 Homogeneity and yield

The homogeneity of the CERMET resistors over a 256 strip detector is shown in Fig. 9. Every 10th resistor was measured on a needle probe station. Non of them exhibited a mal-function due to broken resistor lines or insufficient contact performance. Obviously there is a left-right increase in the resistor value with a small oscillation. So far it is not clear, whether this comes from the magnetron sputtering profile or a varying composition in the target. The average value was $(2.98 \pm 0.17) \text{ M}\Omega$.

7 Conclusions

A six mask process for fabricating AC-coupled GaAs microstrip detectors with a new type of integrated biasing resistors was developed. Process temperatures do not exceed 300°C in order to risk a degeneration of the Schottky contacts.

Coupling capacitances with different dielectric layers have been integrated onto microstrip detectors. For full size keystone detectors of 6 cm length and $80 \mu\text{m}$ pitch, the corresponding values of the coupling capacitance were 200 pF and 370 pF for SiO_2 and $\text{SiO}_2/\text{Si}_3\text{N}_4$, respectively. The frequency dependence of the integrated capacitors is almost as good as an external C-chip. Only a weak decrease of the capacitance above 100 kHz was observed.

The measurements have shown that the electrical properties of the $2.47 \text{ M}\Omega$ CERMET resistors are quite reasonable and meet the basic requirements. The sheet resistance of the 121 nm thick rf-sputtered layer at 100 W sputtering power is $78.4 \text{ k}\Omega/\text{sq.}$. It can be varied by the sputtering power. The TCR of $2.5 \times 10^{-3}/^{\circ}\text{C}$ is comparable to that of an external R-Chip that is frequently used for nonintegrated microstrip detectors.

¹ $3,2 \text{ M}\Omega$, Kharkov, Ukraine

It has to be proofed, if the high strip resistance of $150 \Omega/\text{cm}$ significant deteriorates the signal to noise level when amplifiers with fast shaping times are used. The recently fabricated detectors are currently being tested with respect to their charge collection efficiency and position resolution.

8 Acknowledgment

This work has been supported by the BMFT under contract 057FR11I.

References

- [1] E. Barberis et al., Nucl. Instr. and Meth. A 342 (1994) 90-95
- [2] D. Marder et al., Nucl. Instr. and Meth. A 395 (1997) 141-144
- [3] D.Pitzl et al., Nucl. Instr. and Meth. A 348 (1994) 454-460
- [4] E.Petrolo et al., Nucl. Instr. and Meth. A 344 (1994) 194-198
- [5] M.Caccia et al., Nucl. Instr. and Meth. A 260 (1987) 124-131
- [6] W. Gadomski et al., Nucl. Instr. and Meth. A 326 (1993) 239-242
- [7] J. Baines, SCT96 Layout design, (1996)
- [8] R. Irsigler et al., Nucl. Instr. and Meth. A 395 (1997) 71-75
- [9] M.J.Howes et al., "Gallium Arsenide", John Wiley & Sons Ltd. (1985)
- [10] W-C Tsay et al., Nucl. Instr. and Meth. A 351 (1994) 463-465
- [11] J.M.Parsey, "Material Science and Technology", Vol.16, Edt. K. A. Jackson, VCR, (1996), 554
- [12] T.Ohsugi et al., Nucl. Instr. and Meth. A 342 (1994) 16-21
- [13] J.Ellison et al., IEEE Trans. Nucl. Sci. 36 (1989) 267
- [14] P.P.Allport et al., Nucl. Instr. and Meth. A 310 (1991) 155-159
- [15] S.C.Yeh et al., Nucl. Instr. and Meth. A 342 (1994) 49-51
- [16] H.H.Wieder, Properties of Gallium Arsenide, Cpt. 16.18, p.450-451
- [17] J.G.Ameen et al., IBM Techn. Discl. Bull. 19, No.7 (1976) 2485
- [18] J.G.Ameen et al., IBM Techn. Discl. Bull. 21, No.3 (1978) 953
- [19] J.Gow et al., IBM Techn. Discl. Bull. 21, No.12 (1979) 4789

- [20] R. Nagatani, *Journ.Electr.Engineering* 17, No.160 (1980) 38
- [21] H.S.Hoffman, *IEEE Trans. CHMT* 4, No.4, (1981) 387
- [22] J.E.Morris, *Thin Solid Films* 11 (1972) 299
- [23] J.E.Morris, *Rad. Electr. Engineer* 41, No.4 (1971) 163
- [24] H.Steemers et al., *Mat.Res.Sco.Symp.Proc.* 118 (1988) 445
- [25] G.Batignani et al., *Nucl. Instr. and Meth. A* 310 (1991) 161-164

Table 1: Deposition parameters and resistor values

Sputtering power	[W]	100	200
Sputtering time	[s]	250	100
Film thickness	[nm]	121	133
Resistivity	[M Ω]	2.47	4.85
Resistance	[Ω cm]	0.95	3.14
Sheet resistance	[k Ω / \square]	78.4	236
TCR	[$10^{-3}/^{\circ}$ C]	2.5	3.0

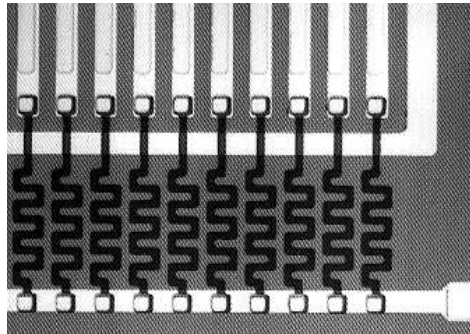


Fig. 1. Integrated CERMET biasing resistors onto GaAs microstrip detectors with a pitch of 50 μm .

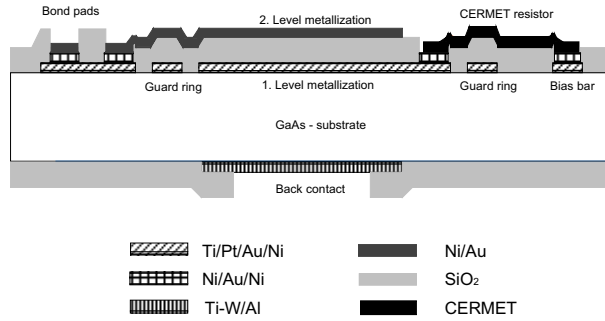


Fig. 2. Cross-section of the AC-coupled GaAs microstrip detector with integrated CERMET biasing resistors.

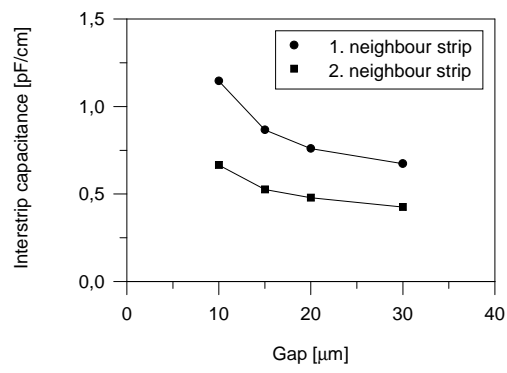


Fig. 3. Interstrip capacitance as a function of gap between strips.

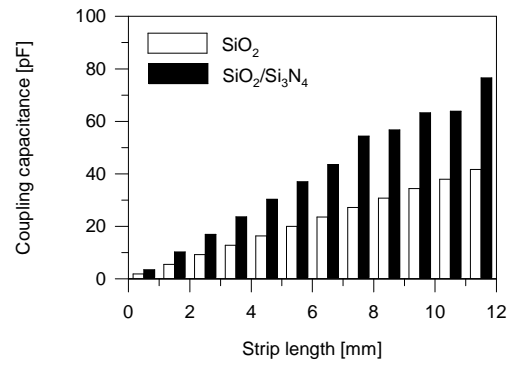


Fig. 4. Coupling capacitances for different dielectrics as a function of strip length.
Strip width: 40 μm

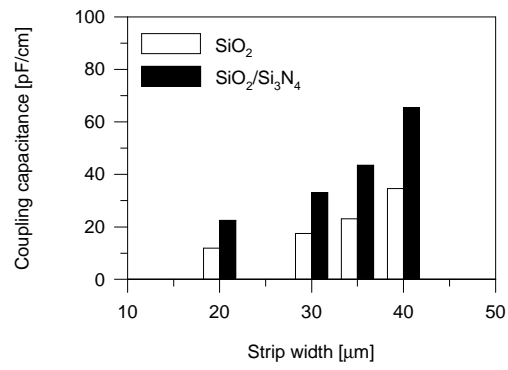


Fig. 5. Coupling capacitance for different dielectrics as a function of strip width.
Strip length: 15 mm

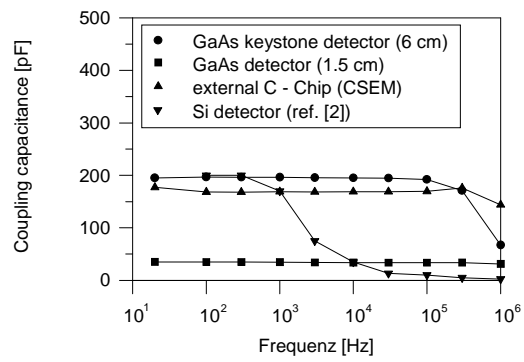


Fig. 6. Coupling capacitance as a function of frequency. In addition to the capacitors integrated onto GaAs detectors, a comparison with an external C-chip and a capacitor integrated onto a silicon detector is shown.

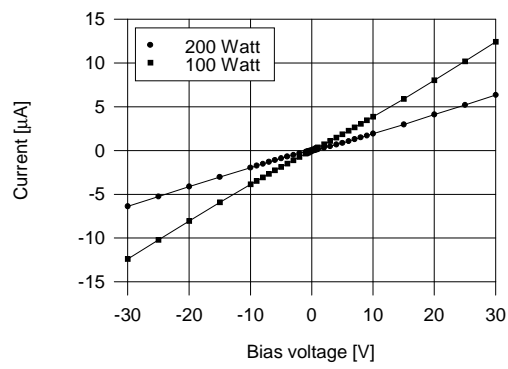


Fig. 7. I-V characteristic for CERMET resistors sputtered at different powers.

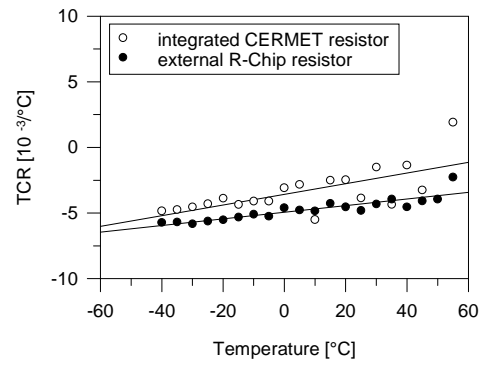


Fig. 8. TCR for an integrated CERMET resistor and an external R-chip resistor

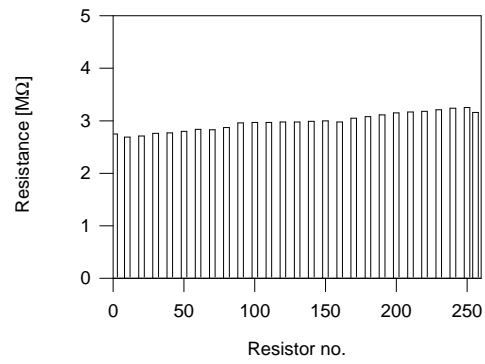


Fig. 9. Homogeneity of the integrated CERMET resistors on a detector with 256 strips